

1 Article

## 2 Insight into the self-assembling properties of a 3 peptergent: a molecular dynamics study

4 Jean-Marc Crowet<sup>1</sup>, Mehmet Nail Nasir<sup>1</sup>, Antoine Deschamps<sup>2</sup>, Vincent Stroobant<sup>3</sup>, Pierre  
5 Morsomme<sup>2</sup>, Magali Deleu<sup>1</sup>, Patrice Soumillion<sup>2</sup>, Laurence Lins<sup>1,\*</sup>

6 <sup>1</sup> Laboratoire de Biophysique Moléculaire aux Interfaces, Gembloux Agro-Bio Tech, University of Liège,  
7 Passage des déportés 2, 5030 Gembloux, Belgium; [jeanmarccrowet@gmail.com](mailto:jeanmarccrowet@gmail.com) (J.M.C.); [mn.nasir@uliege.be](mailto:mn.nasir@uliege.be)  
8 (M.N.N); [Magali.Deleu@Uliege.be](mailto:Magali.Deleu@Uliege.be) (M.D.); [l.lins@Uliege.be](mailto:l.lins@Uliege.be) (L.L.)

9 <sup>2</sup> Institut des Sciences de la Vie, Université catholique de Louvain, 4-5 Place Croix du Sud, 1348 Louvain-la-  
10 Neuve, Belgium; [antoine.deschamps@outlook.com](mailto:antoine.deschamps@outlook.com) (A.D.); [pierre.morsomme@uclouvain.be](mailto:pierre.morsomme@uclouvain.be) (P.M.);  
11 [patrice.soumillion@uclouvain.be](mailto:patrice.soumillion@uclouvain.be) (P.S.)

12 <sup>3</sup> Ludwig Institute for Cancer Research, de Duve Institute and Université Catholique de Louvain, 75 Avenue  
13 Hippocrate, 1200 Brussels, Belgium; [vincent.stroobant@bru.licr.org](mailto:vincent.stroobant@bru.licr.org) (V.S.)

14 \* Correspondence: [l.lins@uliege.be](mailto:l.lins@uliege.be); Tel.: +32-81-622644

15  
16

17 **Abstract:** By manipulating the various physico-chemical properties of amino acids, design of  
18 peptides with specific self-assembling properties has been emerging since more than a decade. In  
19 this context, short peptides possessing detergent properties (so-called “peptergents”) have been  
20 developed to self-assemble into well-ordered nanostructures that can stabilize membrane proteins  
21 for crystallization. In this study, the peptide with “peptergency” properties, called ADA8  
22 extensively described by Zhang *et al.*, is studied by molecular dynamics for its self-assembling  
23 properties in different conditions. In water, it spontaneously forms beta sheets with a  $\beta$  barrel-like  
24 structure. We next simulated the interaction of this peptide with a membrane protein, the  
25 bacteriorhodopsin, in the presence or absence of a micelle of dodecylphosphocholine. According  
26 to the literature, the peptergent ADA8 is thought to generate a belt of  $\beta$  structures around the  
27 hydrophobic helical domain that could help stabilize purified membrane proteins. Molecular  
28 dynamics is here used to challenge this view and to provide further molecular details for the  
29 replacement of detergent molecules around the protein. To our best knowledge, this is the first  
30 molecular mechanism proposed for “peptergency”. In addition, our calculation approach should  
31 serve as a predicting tool for the design of beta peptergent with diverse amphipathic properties.

32 **Keywords:** peptide; self-assembly; molecular dynamics; peptergency; beta structure

33

### 34 1. Introduction

35 By manipulating the various physico-chemical properties of amino acids, the design of  
36 peptides with specific self-assembling properties has been emerging for some years [1]. Due to their  
37 biocompatibility and chemical diversity, peptides are an attractive platform for the design of  
38 various nanostructures, such as nanotubes, vesicles, fibers, micelles or rod-coil structures, that have  
39 potential applications in drug delivery, tissue engineering or surfactants [2,3]. Depending on the  
40 sequence and environment, peptides can self-assemble into ordered structures constrained by non-  
41 covalent interactions, such as electrostatic interactions, hydrophobic interactions, van der Waals  
42 interactions, hydrogen bonds and  $\pi$ -stacking. Particularly, amphiphilic peptides have shown their  
43 ability to self-assemble into a range of nanostructures [3] and behave in some respects like  
44 conventional amphiphilic molecules such as surfactants, detergents and lipids. Amphipathicity can  
45 arise either from peptides containing polar and nonpolar residues distributed regularly along the  
46 peptide [4] or from alkyl chains linked to a hydrophilic peptide.

47 In that way, short peptides possessing detergent properties, so-called “peptergents”, have been  
48 developed in the last decade to self-assemble into well-ordered nanostructures that can stabilize  
49 membrane proteins for crystallization [5]. Three main classes are described in the literature:  
50 amphipathic helical peptides [6], lipopeptides [7–9] and short lipid-like peptides [10–12]. From a  
51 conformational point of view, some of these peptides can adopt  $\alpha$  helical or extended  $\beta$  sheet  
52 structures during their self-assembly. Recently, the Zhang’s group engineered a  $\beta$ -sheet peptide  
53 able to self-assemble and to sequester integral membrane proteins (IMPs) [13]. The peptide is  
54 amphipathic, alternating hydrophobic and hydrophilic residues. It is also methylated at some  
55 amino groups and is grafted with two alkyl chains. It is proposed that the peptide is able to  
56 associate with IMPs in a  $\beta$  barrel-like configuration.

57 There are many detergents available for the solubilization and crystallization of membrane  
58 proteins [14]. However, these detergents need to stabilize the native structure of the protein to  
59 maintain its function and avoid aggregation. Finding the optimal detergents for the protein studied  
60 requires wide screening and depends on the application [12]. New ones are required, and some  
61 peptergents have shown better stabilizing properties than commonly used alkyl chain surfactants  
62 [15]. Even though experimental evidence is available concerning the relative efficacy of peptergents  
63 in solubilizing and stabilizing IMPs [10,11,13,16], little is known about the molecular mechanisms  
64 involved in their interactions with proteins.

65 In this work, we studied the self-assembling properties of a known peptide called ADA8 [3]  
66 (Fig. 1a) using molecular dynamics (MD). In water, this peptide is able to self-assemble as a beta  
67 barrel-like structure. In the presence of an integral membrane protein, the peptide forms a beta belt  
68 around the protein with and without surfactant molecules. To the best of our knowledge, this is the  
69 first time that a molecular mechanism is proposed by MD for “peptergency”. Our calculation  
70 approach should further serve as a predicting tool for the design of beta peptergent with diverse  
71 amphipathic properties, as suggested for a *de novo* designed peptide, ABZ12.

## 72 2. Results

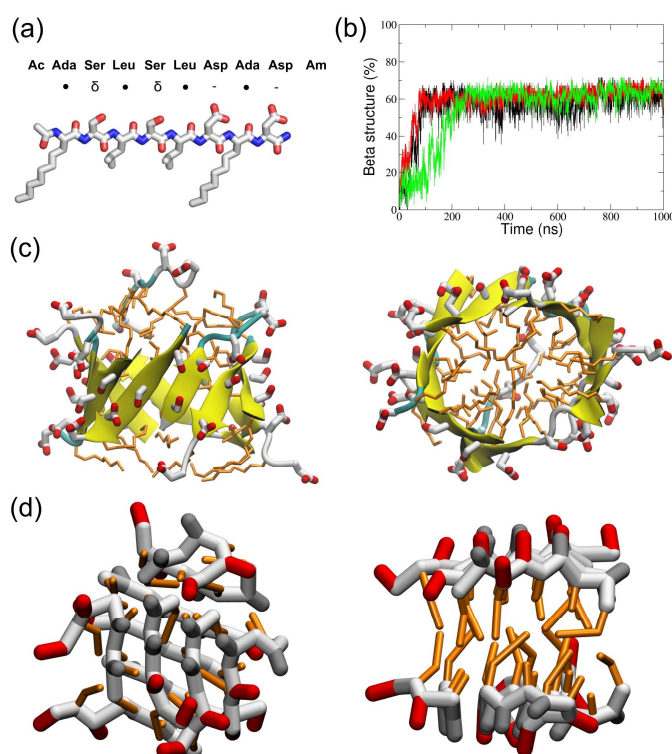
### 73 2.1. Simulations in water

74 Ten ADA8 peptides (fig. 1a) were simulated in water in atomistic (AT) (1  $\mu$ s) and coarse  
75 grained (CG) (10  $\mu$ s) representations to follow their self-assembly (Fig. 1). The black curve of Fig. 1b  
76 shows a rapid increase in the beta structure during AT simulations in water and the beta sheets  
77 formed can be seen in Fig. 1c. These structures are similar to beta barrels with the peptides adopting  
78 amphiphilic beta strand conformations, their hydrophobic residues facing the inside of the barrel.  
79 The strands can be parallel or anti-parallel. The self-assembly has also been simulated in a CG  
80 representation since longer time scales can be achieved. At the end of the CG simulation, we  
81 observed two amphiphilic beta sheets facing each other, with the hydrophobic residues buried  
82 between the sheets (fig. 1d). Polar interactions between sidechains as well as backbone interactions  
83 between the strands are also noticed. To estimate the formation of beta structures, a parameter that  
84 is based on  $C\alpha$  or backbone beads positions has been used (see Methods). As observed in AT  
85 simulations, the peptides are able to adopt a beta conformation along the simulation, as assessed by  
86 the green curve in Fig. 1b and the molecular assembly in Fig. 1d. Though the beta sheet twist  
87 observed in atomistic simulations is not reproduced by the CG model and leads to the formation of  
88 two facing beta sheets instead of a beta barrel. It is worth noting that the MARTINI force field is, in  
89 principle, not designed to sample native conformations [17], especially for beta sheet structures,  
90 since there is no hydrogen bond representation. In the literature, several fibril-forming peptides  
91 have been studied using MARTINI [18,19], such as the aggregation of the Apo C-II amyloid peptide  
92 or the assembly of the protofibrils of amylin. However, beta sheet formation was not observed for  
93 the Apo C-II peptide, and the beta conformation of amylin protofibrils was restrained before  
94 elongation could occur. Nevertheless, Seo *et al.* have observed beta sheet formation with MARTINI,  
95 but they modified the backbone potentials to reproduce structural properties derived from  
96 atomistic simulations [20]. Here, we observed the appearance of beta sheets without any  
97 modification of the force field; this is mainly due to the beta amphipathic nature of the ADA8

98 peptide. Some differences between CG and AT beta sheets were nevertheless observed. CG strands  
 99 in beta sheets are shifted by one residue compared to atomistic beta sheets (Fig. 1d). In the latter,  
 100 the relative positions of the beta strands are defined by hydrogen bonding and the side chains on  
 101 both sheet sides align. In contrast, in CG, the attraction comes from the backbone (BB) beads, and  
 102 the shifted position minimizes the overall BB bead distance between strands. The question of the  
 103 backbone representation in MARTINI was discussed by Marrink *et al.* in 2013; a perspective  
 104 evolution of the force field would be to add charged beads to the backbone in order to reproduce  
 105 the structural preferences of proteins [21].

106 To assess the stability of the beta structure formed, the structure represented on Fig. 1d has  
 107 been transformed to an atomistic resolution and further simulated for 25 ns. This simulation shows  
 108 a small decrease in the beta sheet content with a reorganisation to form a beta barrel (see  
 109 Supplementary Fig. S1). Globally, for all the simulations, the peptides are able to form beta  
 110 structures, which agrees with the literature [13].

111

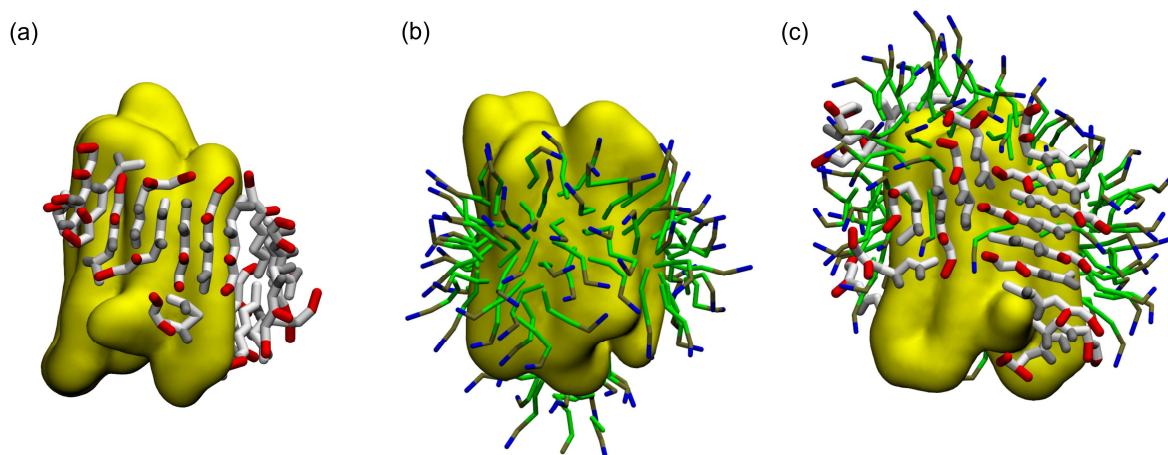


112 **Figure 1. ADA8 peptide structures in water.** (a) Representation of the ADA8 peptide. ●, δ and -  
 113 represent hydrophobic, polar and negatively charged residues, respectively. (b) Percentage of beta  
 114 conformation. The structure is assigned by Stride in AT (black curve) and by using the following  
 115 parameter in CG : a dihedral angle greater than 100° for four following CA atoms and two other  
 116 following CA atoms within 6 Å. The red and green curves correspond to this parameter for AT and  
 117 CG simulations respectively. Conformations at the end of simulations in atomistic and coarse  
 118 grained representations are in panels (c) and (d), respectively; the right panels are an upper view of  
 119 the left panels. AT beta sheets are in yellow in the AT representations. Polar, negatively charged and  
 120 hydrophobic CG residues are represented in gray, red and orange, respectively.

## 121 2.2. Coarse grained simulation of the peptide in the presence of a membrane protein

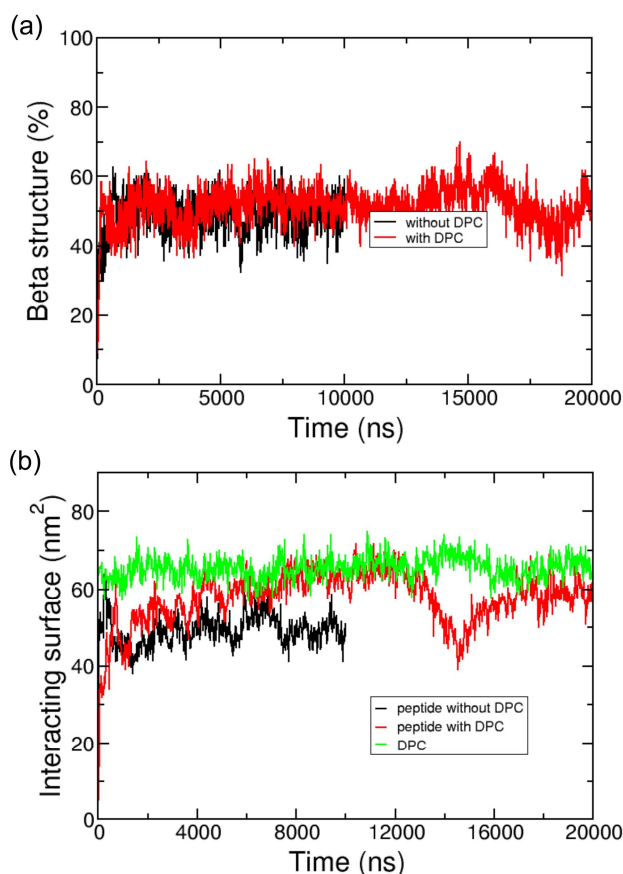
122 ADA8 was shown by Tao *et al.* to be a very efficient peptergent and to solubilize membrane  
 123 proteins such as rhodopsin [13]. Thus, we chose an IMP with a known and well-characterized 3D  
 124 structure, bacteriorhodopsin (BRD). Twenty peptides were simulated in water in the presence of  
 125 one BRD protein over 10 μs in CG representation. Figure 2 represents the peptides interacting with  
 126 BRD at the end of the simulations and shows that the peptides form amphipathic beta sheets at the  
 127 hydrophobic domain of the IMP and present their hydrophilic residues to water. This process can

128 be followed in Fig. 3a, which shows an increase in the beta sheet content during the simulations,  
129 and Fig. 3b, where an increase in the area of the interacting surfaces between the peptides and the  
130 protein is observed. The peptides are rapidly attracted by the protein surface, and through  
131 interactions with BRD, they bury their hydrophobic residues. They form hydrophobic, polar and  
132 backbone interactions between the antiparallel or parallel beta strands (Fig. 2). Once at the protein  
133 surface, the reorganization of the peptides slowly occurs. The protein surface is 115 nm<sup>2</sup> and the  
134 portion covered by the peptides represents about 50 nm<sup>2</sup>. The peptides are also positioned mainly  
135 on the hydrophobic part of the protein. They are not always oriented parallel to the helices axis as  
136 expected for a beta barrel-like organization.



137 **Figure 2. ADA8 peptide organization on the surface of the membrane protein.** The structures  
138 show 20 peptides at the end of the CG simulations when the protein (in yellow) is alone (a) or  
139 covered by DPC (c). The protein surrounded by DPC is shown (b), and this structure was used as a  
140 starting point before the addition of the peptides (c).

141 Figure 2c shows that when DPC is present at the surface of the protein, the peptide is able to  
142 go to the protein surface and form beta sheet structures similar to the situation without DPC.  
143 Furthermore, as the peptide is located on the transmembrane domain of BRD, it displaces DPC  
144 molecules around the hydrophobic core of the protein (Fig. 2c). Figure 3 depicts the beta structure  
145 (Fig.3a) and the surface of the interaction between the peptides (with or without DPC) and the  
146 protein (fig.3b) that are relatively stable along the simulations.



147 **Figure 3. Secondary structure evolution (a) and surface of the interaction (b) of the peptide ADA8**  
 148 **in the presence of a membrane protein with (red lines) and without (black lines) DPC. The**  
 149 **surface of the interaction between DPC and the membrane protein in the presence of the ADA8**  
 150 **peptide is represented in green.**

### 151 3. Discussion

152 In this study, we have analyzed the molecular behavior of ADA8, a well described peptergent,  
 153 for its solubilizing and stabilizing propensity of IMPs by molecular dynamics. The peptide self-  
 154 assembles into beta structures in water and is able to interact with a membrane protein, in  
 155 agreement with the experimental data previously published [3]. In water, the peptide forms  
 156 amphipathic beta sheets that look like  $\beta$ -barrel for the AT representation or as 'sandwich' like  $\beta$ -  
 157 sheets in CG. It is worth noting that the peptides were successfully simulated in atomistic and  
 158 coarse grained representations, validating the CG approach for such amphipathic beta peptides.  
 159 The validation of the CG approach was notably assessed by using reverse transformations: hence,  
 160 AT simulations carried out after reverse transformation showed that the beta sheets formed in CG  
 161 were still stable.

162 When a membrane protein is present, the peptide steadily forms a beta sheet structure at the  
 163 protein surface and is able to displace DPC surfactants. Tao *et al.* proposed a model for the  
 164 organization of the peptides around an IMP [9]. The peptides are thought to generate a beta-barrel  
 165 belt around the hydrophobic helical domain that could help stabilize purified membrane proteins  
 166 [13]. The MD approaches developed in our study challenge this view and provide further molecular  
 167 details for the replacement of detergent molecules around the protein. Although a complete belt  
 168 was not obtained during the course of the simulations, the system tended to move toward this  
 169 configuration.

170 In their work, Tao *et al.* also asked how IMPs are stabilized by beta strand peptides that can  
 171 assemble into beta structures in solution [13]. Our calculations suggest that beta sheet formation is  
 172 favored in water, suggesting a strong peptide/peptide interaction. In the presence of membrane  
 173 proteins, even those solubilized with surfactants, the ADA8 peptide could also form beta sheets at

174 the protein surface. As the peptide/peptide interaction is stronger than that of surfactants, the  
175 former appears to steadily displace surfactants from the protein hydrophobic surface. Since Tao *et*  
176 *al.* showed that their model membrane protein retains its activity, we assumed that the IMP  
177 structure is not restrained by the beta sheet structure. Compared to the assumption of Tao *et al.*, our  
178 calculations suggest that the belt formed around the membrane protein is not 'perfect'. The beta  
179 strands can be parallel or antiparallel and beta sheets perpendicular to the protein  $\alpha$  helices are  
180 observed.

181 Our MD approach could be used to select peptides with 'peptergency' properties, i.e.  
182 amphiphilic peptides with a  $\beta$  sheet structure propensity and the ability to form a  $\beta$  belt-like  
183 structure around an IMP in the presence or absence of detergent molecules. As an example, we  
184 designed a peptide called ABZ12 to be in a  $\beta$  conformation, being composed of residues most  
185 frequently found in  $\beta$  conformation, such as Arg, Val, Ile or Thr [22,23]. A size of 12 amino acids is  
186 also compatible with the width of membrane bilayers and is usually observed for membrane  
187 proteins with a beta barrel fold [24,25]. Hydrophobic amino acids (Val and Ile) alternate with  
188 hydrophilic residues (Arg, Thr, and Ser) to generate amphipathy and promote the formation of beta  
189 strands [4]. Positive charges in the N-terminal part combined with negative charges at the C-  
190 terminal part should allow an antiparallel arrangement while keeping global neutrality. A  
191 fluorescent N-terminal cap is added in the form of an aminobenzoyl group for experimental  
192 purposes. ATR-infrared spectroscopy assays on the peptide (see Supplementary Fig. S3) shows a  
193 peak at approximately 1630  $\text{cm}^{-1}$ , characteristic of  $\beta$ -sheet conformations. According to what was  
194 carried out for ADA8, CG simulations of the system IMP/ABZ12 in the presence or absence of DPC  
195 molecules were calculated. As shown on Fig. S4, the same molecular picture is obtained; ABZ12  
196 forms a beta belt around the membrane protein and displaces detergent molecules when they are  
197 present, suggesting a peptergent-like behavior. Actually, the detergents moved to more apical  
198 regions of the protein in the presence of the peptides. The contact surface between DPC and the  
199 protein decreased by at least 10  $\text{nm}^2$  (Fig. S5). Preliminary experimental results of FRET assays with  
200 ABZ12 show fluorescence energy transfer between the IMP and the aminobenzoic acid group of  
201 ABZ12 (data not shown), suggesting a direct interaction between ABZ12 and the protein. Future  
202 experimental investigations on the ability of ABZ12 to solubilize membrane proteins should help to  
203 assess its 'peptergency' potential.

204 In conclusion, our MD approach using atomistic and coarse grained representations suggest  
205 that one possible mechanism for membrane proteins to be solubilized by  $\beta$  amphipathic self-  
206 assembling peptides is the formation of a belt-like structure around the IMP. This belt is not a  
207 perfect  $\beta$  barrel, contrary to what was suggested previously. To our best knowledge, this is the first  
208 molecular insight proposed for "peptergency".

## 209 4. Materials and Methods

### 210 4.1. Peptide synthesis

211 The ABZ12 peptide was synthesized by conventional solid phase peptide synthesis using Fmoc  
212 for transient  $\text{NH}_2$ -terminal protection and was characterized using mass spectrometry. The peptide  
213 was lyophilized and resolubilized in DMSO at a final concentration of 10 % (w/v) peptide as a stock  
214 solution. Before mixing with water, the peptide solution in DMSO was first diluted to 0.5% to avoid  
215 insolubility.

### 216 4.2. Fourier Transform Infra Red (FTIR) experiments

217 The infrared spectra were measured using a Bruker Equinox 55 spectrometer (Karlsruhe,  
218 Germany) equipped with a liquid nitrogen-cooled DTGS detector. The spectra were recorded from  
219 4,000 to 750  $\text{cm}^{-1}$  in ATR mode after 1,024 scans at 4  $\text{cm}^{-1}$  resolution and at a two-level zero filling.  
220 During the data acquisition, the spectrometer was continuously purged with filtered dried nitrogen.  
221 For sample measurement, the peptide solubilized in DMSO was deposited on a germanium plate, and  
222 DMSO was evaporated under the  $\text{N}_2$  flux for approximately 5 hours. Reference spectra of the

223 germanium plate were automatically recorded and subtracted from the sample spectrum. The  
224 resulting spectrum was then smoothed using the Savitzky-Golay algorithm available in the OPUS  
225 software.

#### 226 4.3. Molecular systems studied by MD

227 Two peptides were studied by molecular dynamics (MD); their properties are depicted in Fig. 1  
228 and S2. The ADA8 peptide is described in Tao *et al.* [13]; it contains two non-natural 2-aminodecanoic  
229 acids (ADA) and is acetylated at the N-terminus and amidated at the C-terminus (Fig. 1b) [13]. The  
230 ABZ12 peptide was designed as an example for this study; it is capped at the N-terminus by an  
231 aminobenzoic acid and is free at the C-terminus. The peptides have been modeled in an extended beta  
232 conformation based on experimental data (FTIR). The force field Gromos96 54a7 (G54a7) [26] was  
233 used during this study. The ABZ topology came from a study by Song *et al.* in 2010 [27], and the ADA  
234 topology was derived from the ILE amino acid. The SPC model [28] was used to simulate water. The  
235 MARTINI force field [17,29] has been used for coarse grained (CG) simulations. The ABZ residue was  
236 replaced by a PHE residue. The membrane protein used was bacteriorhodopsin (PDBID: 1PY6), and  
237 its tertiary structure has been maintained with the SAHBNET network [30].

#### 238 4.4. Atomistic molecular dynamics

239 Simulations were performed with the G54a7 force field [26]. All the systems studied (see  
240 Supplementary Table S1) were first minimized by steepest descent for 5,000 steps. Then, a 1 ns  
241 simulation with the peptides under position restraints was run before the production simulations  
242 were performed. Periodic boundary conditions (PBC) were used with a 2 fs time step. All the systems  
243 were solvated with SPC water [28] and the dynamics were carried out under NPT conditions (298 K  
244 and 1 bar). The temperature was maintained using the v-rescale method [31] with  $\tau_T = 0.2$  ps, and an  
245 isotropic pressure was maintained using the Parrinello-Rahman barostat [32] with a compressibility of  
246  $4.5 \times 10^5$  (1/bar) and  $\tau_P = 1$  ps. Electrostatic interactions were treated using the particle mesh Ewald  
247 (PME) method [33]. Van der Waals and electrostatic interactions were treated with a 1.0 nm cut-off.  
248 Bond lengths were maintained with the LINCS algorithm [34]. Trajectories were performed and  
249 analyzed with GROMACS 4.5.4 tools as well as with homemade scripts and software. MDAnalysis  
250 was also used [35]. The 3D structures were analyzed with both the PyMOL [36] and VMD [37]  
251 softwares. The secondary structures were computed with STRIDE [38].

#### 252 4.5. Coarse grained molecular dynamics

253 The peptide models were converted to a CG representation suitable for the MARTINI force field  
254 [17], and the coarse grained peptides were placed in a simulation box with water (see Supplementary  
255 Table S1). A total of 5,000 steps of steepest-descent energy minimization were performed to remove  
256 any steric clashes, and production simulations were run. Temperature and pressure were set at 298 K  
257 and 1 bar using the weak coupling Berendsen algorithm [39] with  $\tau_T = 1$  ps and  $\tau_P = 1$  ps. Pressure  
258 was coupled isotropically. Non-bonded interactions were computed up to 1.2 nm with the shift  
259 method. Electrostatic interactions were treated with  $\epsilon = 15$ . The compressibility was  $3 \times 10^4$  (1/bar).  
260 Coarse grained simulations were carried out using Gromacs 4.5.4. [40] To compare the structure  
261 evolution between AT and CG, we had to compute a parameter representing the beta structure in CG.  
262 Hence, as the backbone is only represented by one bead in CG, it is not possible to compute the  
263 phi/psi angles. A dihedral angle greater than  $100^\circ$  and the proximity of two other bonded backbone  
264 beads within 6 Å are used to consider a bead to be part of a beta sheet structure. These values have  
265 been taken from atomistic simulations and allow for the calculation of the beta structure content with  
266 enough precision (see Fig. 1b).

267 **Supplementary Materials:** Supplementary materials can be found at [www.mdpi.com/link](http://www.mdpi.com/link).

268 **Acknowledgments:** We would like to thank the FNRS (PDR grant T.1003.14; CDR grant J.0114.18), the Belgian  
269 Program on Interuniversity Attraction Poles initiated by the Federal Office for Scientific, Technical and  
270 Cultural Affairs (IAP P7/44 iPros) and ERA NET CoBiotech (Bestbiosurf project) for financial support. MD and

271 LL are Senior Research Associates for the Fonds National de la Recherche Scientifique (FRS-FNRS). JMC and  
272 MNN were supported by the ARC FIELD project. Partial computational resources of the lab were provided by  
273 the "Consortium des Équipements de Calcul Intensif" (CECI) and were funded by the F.R.S.-FNRS under  
274 Grant No. 2.5020.11.

275 **Author Contributions:** J-M.C. and L.L. designed the calculations and experiments, JMC performed all  
276 calculations and analyses; JMC and LL drafted the manuscript and figures. A.D., P.M. and P.S. designed the  
277 ABZ12 peptide. Infrared spectroscopy was carried out by M.N.N. and the peptide synthesis was carried out by  
278 V.S. All authors reviewed the manuscript.

279 **Conflicts of Interest:** "The authors declare no conflict of interest."

## 280 References

- 281 1. Lakshmanan, A.; Zhang, S.; Hauser, C. A. E. Short self-assembling peptides as building blocks for  
282 modern nanodevices. *Trends Biotechnol.* **2012**, *30*, 155–65, doi:10.1016/j.tibtech.2011.11.001.
- 283 2. Mandal, D.; Nasrolahi Shirazi, A.; Parang, K. Self-assembly of peptides to nanostructures. *Org. Biomol.*  
284 *Chem.* **2014**, *12*, 3544–61, doi:10.1039/c4ob00447g.
- 285 3. Zhang, S.; Marini, D. M.; Hwang, W.; Santoso, S. Design of nanostructured biological materials through  
286 self-assembly of peptides and proteins. *Curr. Opin. Chem. Biol.* **2002**, *6*, 865–71.
- 287 4. Xiong, H.; Buckwalter, B. L.; Shieh, H. M.; Hecht, M. H. Periodicity of polar and nonpolar amino acids is  
288 the major determinant of secondary structure in self-assembling oligomeric peptides. *Proc. Natl. Acad. Sci.*  
289 *U. S. A.* **1995**, *92*, 6349–53.
- 290 5. Zhang, Q.; Tao, H.; Hong, W.-X. New amphiphiles for membrane protein structural biology. *Methods*  
291 **2011**, *55*, 318–23, doi:10.1016/j.ymeth.2011.09.015.
- 292 6. Schafmeister, C. E.; Miercke, L. J.; Stroud, R. M. Structure at 2.5 Å of a designed peptide that maintains  
293 solubility of membrane proteins. *Science* **1993**, *262*, 734–8.
- 294 7. McGregor, C.-L.; Chen, L.; Pomroy, N. C.; Hwang, P.; Go, S.; Chakrabartty, A.; Privé, G. G. Lipopeptide  
295 detergents designed for the structural study of membrane proteins. *Nat. Biotechnol.* **2003**, *21*, 171–6,  
296 doi:10.1038/nbt776.
- 297 8. Wang, X.; Huang, G.; Yu, D.; Ge, B.; Wang, J.; Xu, F.; Huang, F.; Xu, H.; Lu, J. R. Solubilization and  
298 stabilization of isolated photosystem I complex with lipopeptide detergents. *PLoS One* **2013**, *8*, e76256,  
299 doi:10.1371/journal.pone.0076256.
- 300 9. Ho, D. N.; Pomroy, N. C.; Cuesta-Seijo, J. A.; Privé, G. G. Crystal structure of a self-assembling  
301 lipopeptide detergent at 1.20 Å. *Proc. Natl. Acad. Sci. U. S. A.* **2008**, *105*, 12861–6,  
302 doi:10.1073/pnas.0801941105.
- 303 10. Kiley, P.; Zhao, X.; Vaughn, M.; Baldo, M. a; Bruce, B. D.; Zhang, S. Self-assembling peptide detergents  
304 stabilize isolated photosystem I on a dry surface for an extended time. *PLoS Biol.* **2005**, *3*, e230,  
305 doi:10.1371/journal.pbio.0030230.
- 306 11. Zhao, X.; Nagai, Y.; Reeves, P. J.; Kiley, P.; Khorana, H. G.; Zhang, S. Designer short peptide surfactants  
307 stabilize G protein-coupled receptor bovine rhodopsin. *Proc. Natl. Acad. Sci. U. S. A.* **2006**, *103*, 17707–12,  
308 doi:10.1073/pnas.0607167103.
- 309 12. Corin, K.; Baaske, P.; Ravel, D. B.; Song, J.; Brown, E.; Wang, X.; Wienken, C. J.; Jerabek-Willemsen, M.;  
310 Duhr, S.; Luo, Y.; Braun, D.; Zhang, S. Designer lipid-like peptides: A class of detergents for studying  
311 functional olfactory receptors using commercial cell-free systems. *PLoS One* **2011**, *6*, e25067,  
312 doi:10.1371/journal.pone.0025067.
- 313 13. Tao, H.; Lee, S. C.; Moeller, A.; Roy, R. S.; Siu, F. Y.; Zimmermann, J.; Stevens, R. C.; Potter, C. S.;  
314 Carragher, B.; Zhang, Q. Engineered nanostructured  $\beta$ -sheet peptides protect membrane proteins. *Nat.*  
315 *Methods* **2013**, *10*, 759–761, doi:10.1038/nmeth.2533.
- 316 14. Carpenter, E. P.; Beis, K.; Cameron, A. D.; Iwata, S. Overcoming the challenges of membrane protein  
317 crystallography. *Curr. Opin. Struct. Biol.* **2008**, *18*, 581–6, doi:10.1016/j.sbi.2008.07.001.
- 318 15. Ge, B.; Yang, F.; Yu, D.; Liu, S.; Xu, H. Designer amphiphilic short peptides enhance thermal stability of  
319 isolated photosystem-I. *PLoS One* **2010**, *5*, e10233, doi:10.1371/journal.pone.0010233.
- 320 16. Moeller, A.; Lee, S. C.; Tao, H.; Speir, J. A.; Chang, G.; Urbatsch, I. L.; Potter, C. S.; Carragher, B.; Zhang,  
321 Q. Distinct conformational spectrum of homologous multidrug ABC transporters. *Structure* **2015**, *23*, 450–  
322 60, doi:10.1016/j.str.2014.12.013.
- 323 17. Monticelli, L.; Kandasamy, S. K.; Periole, X.; Larson, R. G.; Tieleman, D. P.; Marrink, S. The MARTINI  
324 Coarse-Grained Force Field: Extension to Proteins. *J. Chem. Theory Comput.* **2008**, *4*, 819–834,  
325 doi:10.1021/ct700324x.
- 326 18. Hung, A.; Yarovsky, I. Inhibition of peptide aggregation by lipids: insights from coarse-grained  
327 molecular simulations. *J. Mol. Graph. Model.* **2011**, *29*, 597–607, doi:10.1016/j.jmglm.2010.11.001.
- 328 19. Sørensen, J.; Periole, X.; Skeby, K. K.; Marrink, S.-J.; Schiøtt, B. Protofibrillar Assembly Toward the  
329 Formation of Amyloid Fibrils. *J. Phys. Chem. Lett.* **2011**, *2*, 2385–2390, doi:10.1021/jz2010094.

- 330 20. Seo, M.; Rauscher, S.; Pomès, R.; Tieleman, D. P. Improving Internal Peptide Dynamics in the Coarse-  
331 Grained MARTINI Model: Toward Large-Scale Simulations of Amyloid- and Elastin-like Peptides. *J.*  
332 *Chem. Theory Comput.* **2012**, *8*, 1774–1785, doi:10.1021/ct200876v.
- 333 21. Marrink, S. J.; Tieleman, D. P. Perspective on the Martini model. *Chem. Soc. Rev.* **2013**, *42*, 6801–22,  
334 doi:10.1039/c3cs60093a.
- 335 22. Bhattacharjee, N.; Biswas, P. Position-specific propensities of amino acids in the  $\beta$ -strand. *BMC Struct.*  
336 *Biol.* **2010**, *10*, 29, doi:10.1186/1472-6807-10-29.
- 337 23. Malkov, S. N.; Zivković, M. V.; Beljanski, M. V.; Hall, M. B.; Zarić, S. D. A reexamination of the  
338 propensities of amino acids towards a particular secondary structure: classification of amino acids based  
339 on their chemical structure. *J. Mol. Model.* **2008**, *14*, 769–75, doi:10.1007/s00894-008-0313-0.
- 340 24. Wimley, W. C. The versatile beta-barrel membrane protein. *Curr. Opin. Struct. Biol.* **2003**, *13*, 404–11.
- 341 25. Jackups, R.; Liang, J. Interstrand pairing patterns in beta-barrel membrane proteins: the positive-outside  
342 rule, aromatic rescue, and strand registration prediction. *J. Mol. Biol.* **2005**, *354*, 979–93,  
343 doi:10.1016/j.jmb.2005.09.094.
- 344 26. Schmid, N.; Eichenberger, A. P.; Choutko, A.; Riniker, S.; Winger, M.; Mark, A. E.; van Gunsteren, W. F.  
345 Definition and testing of the GROMOS force-field versions 54A7 and 54B7. *Eur. Biophys. J.* **2011**, *40*, 843–  
346 56, doi:10.1007/s00249-011-0700-9.
- 347 27. Song, B.; Kibler, P.; Malde, A.; Kodukula, K.; Galande, A. K. Design of short linear peptides that show  
348 hydrogen bonding constraints in water. *J. Am. Chem. Soc.* **2010**, *132*, 4508–9, doi:10.1021/ja905341p.
- 349 28. Hermans, J.; Berendsen, H. J. C.; Van Gunsteren, W. F.; Postma, J. P. M. A consistent empirical potential  
350 for water-protein interactions. *Biopolymers* **1984**, *23*, 1513–1518, doi:10.1002/bip.360230807.
- 351 29. Marrink, S. J.; Risselada, H. J.; Yefimov, S.; Tieleman, D. P.; de Vries, A. H. The MARTINI force field:  
352 coarse grained model for biomolecular simulations. *J. Phys. Chem. B* **2007**, *111*, 7812–24,  
353 doi:10.1021/jp071097f.
- 354 30. Dony, N.; Crowet, J. M.; Joris, B.; Brasseur, R.; Lins, L. SAHBNET, an Accessible Surface-Based Elastic  
355 Network: An Application to Membrane Protein. *Int. J. Mol. Sci.* **2013**, *14*, 11510–26,  
356 doi:10.3390/ijms140611510.
- 357 31. Bussi, G.; Donadio, D.; Parrinello, M. Canonical sampling through velocity rescaling. *J. Chem. Phys.* **2007**,  
358 *126*, 014101, doi:10.1063/1.2408420.
- 359 32. Parrinello, M. Polymorphic transitions in single crystals: A new molecular dynamics method. *J. Appl.*  
360 *Phys.* **1981**, *52*, 7182, doi:10.1063/1.328693.
- 361 33. Essmann, U.; Perera, L.; Berkowitz, M. L.; Darden, T.; Lee, H.; Pedersen, L. G. A smooth particle mesh  
362 Ewald method. *J. Chem. Phys.* **1995**, *103*, 8577, doi:10.1063/1.470117.
- 363 34. Hess, B.; Bekker, H.; Berendsen, H. J. C.; Fraaije, J. G. E. M. LINCS: A linear constraint solver for  
364 molecular simulations. *J. Comput. Chem.* **1997**, *18*, 1463–1472, doi:10.1002/(SICI)1096-  
365 987X(199709)18:12<1463::AID-JCC4>3.0.CO;2-H.
- 366 35. Michaud-Agrawal, N.; Denning, E. J.; Woolf, T. B.; Beckstein, O. MDAAnalysis: a toolkit for the analysis of  
367 molecular dynamics simulations. *J. Comput. Chem.* **2011**, *32*, 2319–27, doi:10.1002/jcc.21787.
- 368 36. Schrödinger, L. The PyMOL Molecular Graphics System, Version 1.3 2010.
- 369 37. Humphrey, W.; Dalke, A.; Schulten, K. VMD: visual molecular dynamics. *J. Mol. Graph.* **1996**, *14*, 33–8,  
370 27–8.
- 371 38. Frishman, D.; Argos, P. Incorporation of non-local interactions in protein secondary structure prediction  
372 from the amino acid sequence. *Protein Eng.* **1996**, *9*, 133–42.
- 373 39. Berendsen, H. J. C.; Postma, J. P. M.; van Gunsteren, W. F.; DiNola, a; Haak, J. R. Molecular dynamics  
374 with coupling to an external bath. *J. Chem. Phys.* **1984**, *81*, 3684–3690, doi:10.1063/1.448118.
- 375 40. Hess, B.; Kutzner, C.; van der Spoel, D.; Lindahl, E. GROMACS 4: Algorithms for Highly Efficient, Load-  
376 Balanced, and Scalable Molecular Simulation. *J. Chem. Theory Comput.* **2008**, *4*, 435–447,  
377 doi:10.1021/ct700301q.